fibroblasts could be used as feeder cells in the culture of human iPSC [32].

Almost the entire process of reprogramming in iPSC remains poorly understood. It is still unclear whether iPSC reprogramming is equal to nuclear transplantation, which showed that the somatic nucleus reacquired totipotency. The following factors imply that multiple processes exist in reprogramming: the expression of stem cell-related genes differs between iPSC clones [33], and "memories" of the parent cells remain. It has been reported that trichostatin A, a histone deacetylase inhibitor, is a factor that promotes this phenomenon [34]. The necessity of using it under strictly controlled temporal and quantitative requirements indicates the preciseness of its mechanism.

Direct conversion to differentiated cells

The phenomenon termed direct conversion to differentiated cells is a novel occurrence recently reported to occur in several organs. Although many researchers have searched for the master gene, such as MyoD, that can induce formation of skeletal muscle cells from fibroblasts, no such gene has been discovered. However, because the use of four genes allows the differentiated cell to have pluripotency, transformation with one batch of gene transfer is been investigated. A first report described successful differentiation of pancreatic exocrine cells into insulin-secreting beta-like cells by the transfer of three genes (Ngn3/Pdx1/MafA) [35]. Another report documented successful induction of cells expressing myocardial cell structural proteins through the transfer of Gata4/Tbx5/Baf60c into mouse mesodermal cells [36]. According to later reports, functional neurons can be induced by transferring Asc11/Brn2/Myt11 into fibroblasts [37], and myocardial cells can be induced by transferring Gata4/Tbx5/Mef2c into fibroblasts [38]. Thus far, the possibility that these cells only caused specific gene expression that exists in the lower area of transgenes cannot be denied. Functional and quantitative assessments of induced cells produced by direct reprogramming are required to determine their application in the clinical setting.

Somatic stem cells

It was long believed that cardiomyocytes were in a state of terminal differentiation in adults and that the heart cannot heal itself or restore its homeostatic functions. These properties led researchers in cardiac regeneration to increased interest in somatic stem cells, including bone-marrow-derived stem/progenitor cells, mesenchymal stem cells, and adipose-derived stem cells. Because cells derived from fetal-related tissue (including the amnion, umbilical cord, and placenta) contain a multipotent population that shows plasticity, many organizations, institutes, and companies run banking systems for these cells. Transplantation of amniocytes caused cardiac regeneration in myocardial infarction in rats [39]. On the other hand, other researchers have continually asserted the heart has regenerative properties. Recently, clear evidence that cardiomyocytes can be reborn in the adult heart was reported. This evidence was based on cardiomyocyte age estimation by measuring carbon-14, which was generated by nuclear weapons testing during the Cold War [40]. The impetus for the expansion of this field of study was the reporting of a method that was apparently based on embryonic bodies [41]: by forming a sphere with cardiac-tissue-derived cells, a group of nearly undifferentiated cells could be enriched. Subsequently, several groups reported that stem cells and precursor cells exist in the heart. Several profiles were reported for these cells, including c-kit (+) [42], sca-1 (+) [43], and side population cells [44]. Whether this means that we are observing the process of differentiation as it develops or that multiple stem cell systems exist is an issue that needs to be addressed. Matsubara et al. [45], who reported that murine sca-1 (+) cells could be cardiac stem cells (CSC), performed a detailed preclinical study in pigs to treat ischemic heart disease [46] and are directing the world's first clinical trial using CSC. This clinical trial targets patients with severe chronic ischemic heart failure whose left ventricular ejection fraction is <35%. The method involves intramuscular injection of CSC during coronary artery bypass grafting. The injected stem cells are isolated from cardiac tissue collected during a previous biopsy from the right ventricular septal region. During cell culture, recombinant basic fibroblast growth factor (bFGF) is used rather than xenogeneic materials, and blood serum is obtained from autologous blood. The cells are injected through the epicardium, and the injection sites are covered with a basic sustained-release gelatin sheet of bFGF. Patients are not randomized, and six cases are scheduled for an open-label phase I/IIa clinical trial, with a planned 1-year follow-up study. It is assumed that after this trial, cases will accumulate in multifacility clinical studies and that this method will develop into a highly advanced medical technology.

Chemical pharmacology is faced with difficulty finding new classes of drugs despite increasing budgets. Cells and tissues, therefore, are likely to become important medical treatments. Moreover, integrated therapy of ventricular assist device (VAD) and regenerative medicine should have great potential to treat severe heart failure (Fig. 4). Although implantable VADs are being used with excellent prognosis, many issues remain; for example, right ventricular failure, infection, thrombosis, and device mechanical failure. A market report on VAD anticipates that the "bridge to recovery (BTR)" strategy will constitute more

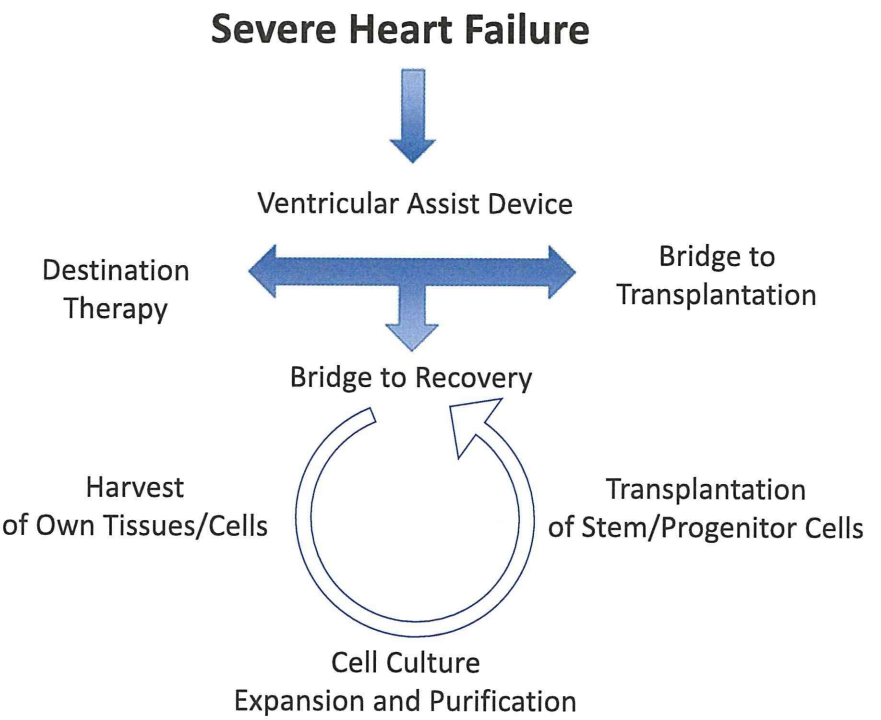

Fig. 4 Integrated strategy to heart failure

than half of future VAD therapy. The emerging field of regenerative medicine will surely accelerate the trend to BTR therapy.

References

1. Kitajima T, Sakuragi M, Hasuda H, Ozu T, Ito Y. A chimeric epidermal growth factor with fibrin affinity promotes repair of injured keratinocyte sheets. Acta Biomater. 2009;5:2623–32.
2. Ohkawara N, Ueda H, Shinozaki S, Kitajima T, Ito Y, Asaoka H, Kawakami A, Kaneko E, Shimokado K. Hepatocyte growth factor fusion protein having collagen-binding activity (CBD-HGF) accelerates re-endothelialization and intimal hyperplasia in balloon-injured rat carotid artery. J Atheroscler Thromb. 2007;14:185–91.
3. Mironov V, Trusk T, Kasyanov V, Little S, Swaja R, Markwald R. Biofabrication: a 21st century manufacturing paradigm. Biofabrication. 2009;1:022001.
4. Jakab K, Norotte C, Marga F, Murphy K, Vunjak-Novakovic G, Forgacs G. Tissue engineering by self-assembly and bio-printing of living cells. Biofabrication. 2010;2:022001.
5. Visconti RP, Kasyanov V, Gentile C, Zhang J, Markwald RR, Mironov V. Towards organ printing: engineering an intra-organ branched vascular tree. Expert Opin Biol Ther. 2010;10:409–20.
6. Nishiyama Y, Nakamura M, Henmi C, Yamaguchi K, Mochizuki S, Nakagawa H, Takiura K. Development of a three-dimensional bioprinter: construction of cell supporting structures using hydrogel and state-of-the-art inkjet technology. J Biomech Eng. 2009;131:035001.
7. Norotte C, Marga FS, Niklason LE, Forgacs G. Scaffold-free vascular tissue engineering using bioprinting. Biomaterials. 2009;30:5910–7.
8. Iwami K, Noda T, Ishida K, Morishima K, Nakamura M, Umeda N. Bio rapid prototyping by extruding/aspirating/refilling thermoreversible hydrogel. Biofabrication. 2010;2:014108.
9. Shimizu T, Yamato M, Kikuchi A, Okano T. Two-dimensional manipulation of cardiac myocyte sheets utilizing temperature-responsive culture dishes augments the pulsatile amplitude. Tissue Eng. 2001;7:141–51.
10. Shimizu T, Sekine H, Yamato M, Okano T. Cell sheet-based myocardial tissue engineering: new hope for damaged heart rescue. Curr Pharm Des. 2009;15:2807–14.
11. Miyagawa S, Saito A, Sakaguchi T, Yoshikawa Y, Yamauchi T, Imanishi Y, Kawaguchi N, Teramoto N, Matsuura N, Iida H, Shimizu T, Okano T, Sawa Y. Impaired myocardium regeneration with skeletal cell sheets—a preclinical trial for tissue-engineered regeneration therapy. Transplantation. 2010;90:364–72.
12. Hida N, Nishiyama N, Miyoshi S, Kira S, Segawa K, Uyama T, Mori T, Miyado K, Ikegami Y, Cui C, Kiyono T, Kyo S, Shimizu T, Okano T, Sakamoto M, Ogawa S, Umezawa A. Novel cardiac precursor-like cells from human menstrual blood-derived mesenchymal cells. Stem Cells. 2008;26:1695–704.
13. Fedak PW. Cardiac progenitor cell sheet regenerates myocardium and renews hope for translation. Cardiovasc Res. 2010;87:8–9.
14. Kobayashi H, Shimizu T, Yamato M, Tono K, Masuda H, Asahara T, Kasanuki H, Okano T. Fibroblast sheets co-cultured with endothelial progenitor cells improve cardiac function of infarcted hearts. J Artif Organs. 2008;11:141–7.
15. Ott HC, Matthiesen TS, Goh SK, Black LD, Kren SM, Netoff TI, Taylor DA. Perfusion-decellularized matrix: using nature's platform to engineer a bioartificial heart. Nat Med. 2008;14:213–21.
16. Wainwright JM, Czajka CA, Patel UB, Freytes DO, Tobita K, Gilbert TW, Badylak SF. Preparation of cardiac extracellular matrix from an intact porcine heart. Tissue Eng Part C Methods. 2010;16:525–32.
17. Soto-Gutierrez A, Zhang L, Medberry C, Fukumitsu K, Faulk D, Jiang H, Reing J, Gramignoli R, Komori J, Ross M, Nagaya M, Lagasse E, Stolz D, Strom SC, Fox IJ, Badylak SF.

A Whole-organ regenerative medicine approach for liver replacement. Tissue Eng Part C Methods 2011.
18. Wernig M, Zhao JP, Pruszak J, Hedlund E, Fu D, Soldner F, Broccoli V, Constantine-Paton M, Isacson O, Jaenisch R. Neurons derived from reprogrammed fibroblasts functionally integrate into the fetal brain and improve symptoms of rats with Parkinson's disease. Proc Natl Acad Sci USA. 2008;105:5856–61.
19. Hanna J, Wernig M, Markoulaki S, Sun CW, Meissner A, Cassady JP, Beard C, Brambrink T, Wu LC, Townes TM, Jaenisch R. Treatment of sickle cell anemia mouse model with iPS cells generated from autologous skin. Science. 2007;318:1920–3.
20. Xu D, Alipio Z, Fink LM, Adcock DM, Yang J, Ward DC, Ma Y. Phenotypic correction of murine hemophilia A using an iPS cell-based therapy. Proc Natl Acad Sci USA. 2009;106:808–13.
21. Hattori F, Chen H, Yamashita H, Tohyama S, Satoh YS, Yuasa S, Li W, Yamakawa H, Tanaka T, Onitsuka T, Shimoji K, Ohno Y, Egashira T, Kaneda R, Murata M, Hidaka K, Morisaki T, Sasaki E, Suzuki T, Sano M, Makino S, Oikawa S, Fukuda K. Nongenetic method for purifying stem cell-derived cardiomyocytes. Nat Methods. 2010;7:61–6.
22. Nakagawa M, Koyanagi M, Tanabe K, Takahashi K, Ichisaka T, Aoi T, Okita K, Mochiduki Y, Takizawa N, Yamanaka S. Generation of induced pluripotent stem cells without Myc from mouse and human fibroblasts. Nat Biotechnol. 2008;26:101–6.
23. Warren L, Manos PD, Ahfeldt T, Loh YH, Li H, Lau F, Ebina W, Mandal PK, Smith ZD, Meissner A, Daley GQ, Brack AS, Collins JJ, Cowan C, Schlaeger TM, Rossi DJ. Highly efficient reprogramming to pluripotency and directed differentiation of human cells with synthetic modified mRNA. Cell Stem Cell. 2010;7:618–30.
24. Kim D, Kim CH, Moon JI, Chung YG, Chang MY, Han BS, Ko S, Yang E, Cha KY, Lanza R, Kim KS. Generation of human induced pluripotent stem cells by direct delivery of reprogramming proteins. Cell Stem Cell. 2009;4:472–6.
25. Maherali N, Hochedlinger K. Tgfbeta signal inhibition cooperates in the induction of iPSCs and replaces Sox2 and cMyc. Curr Biol. 2009;19:1718–23.
26. Feng B, Jiang J, Kraus P, Ng JH, Heng JC, Chan YS, Yaw LP, Zhang W, Loh YH, Han J, Vega VB, Cacheux-Rataboul V, Lim B, Lufkin T, Ng HH. Reprogramming of fibroblasts into induced pluripotent stem cells with orphan nuclear receptor Esrrb. Nat Cell Biol. 2009;11:197–203.
27. Heng JC, Feng B, Han J, Jiang J, Kraus P, Ng JH, Orlov YL, Huss M, Yang L, Lufkin T, Lim B, Ng HH. The nuclear receptor Nr5a2 can replace Oct4 in the reprogramming of murine somatic cells to pluripotent cells. Cell Stem Cell. 2010;6:167–74.
28. Martin MJ, Muotri A, Gage F, Varki A. Human embryonic stem cells express an immunogenic nonhuman sialic acid. Nat Med. 2005;11:228–32.
29. Li Z, Leung M, Hopper R, Ellenbogen R, Zhang M. Feeder-free self-renewal of human embryonic stem cells in 3D porous natural polymer scaffolds. Biomaterials. 2010;31:404–12.
30. Braam SR, Zeinstra L, Litjens S, Ward-van Oostwaard D, van den BS, van Laake L, Lebrin F, Kats P, Hochstenbach R, Passier R, Sonnenberg A, Mummery CL, et al. Recombinant vitronectin is a functionally defined substrate that supports human embryonic stem cell self-renewal via alphavbeta5 integrin. Stem Cells. 2008;26:2257–65.
31. Olmer R, Haase A, Merkert S, Cui W, Palecek J, Ran C, Kirschning A, Scheper T, Glage S, Miller K, Curnow EC, Hayes ES, Martin U. Long term expansion of undifferentiated human iPS and ES cells in suspension culture using a defined medium. Stem Cell Res. 2010;5:51–64.
32. Takahashi K, Narita M, Yokura M, Ichisaka T, Yamanaka S. Human induced pluripotent stem cells on autologous feeders. PLoS One. 2009;4:e8067.
33. Miura K, Okada Y, Aoi T, Okada A, Takahashi K, Okita K, Nakagawa M, Koyanagi M, Tanabe K, Ohnuki M, Ogawa D, Ikeda E, Okano H, Yamanaka S. Variation in the safety of induced pluripotent stem cell lines. Nat Biotechnol. 2009;27:743–5.
34. Kishigami S, Van Thuan N, Hikichi T, Ohta H, Wakayama S, Mizutani E, Wakayama T. Epigenetic abnormalities of the mouse paternal zygotic genome associated with microinsemination of round spermatids. Dev Biol. 2006;289:195–205.
35. Zhou Q, Brown J, Kanarek A, Rajagopal J, Melton DA. In vivo reprogramming of adult pancreatic exocrine cells to beta-cells. Nature. 2008;455:627–32.
36. Takeuchi JK, Bruneau BG. Directed transdifferentiation of mouse mesoderm to heart tissue by defined factors. Nature. 2009;459:708–11.
37. Vierbuchen T, Ostermeier A, Pang ZP, Kokubu Y, Sudhof TC, Wernig M. Direct conversion of fibroblasts to functional neurons by defined factors. Nature. 2010;463:1035–41.
38. Ieda M, Fu JD, Delgado-Olguin P, Vedantham V, Hayashi Y, Bruneau BG, Srivastava D. Direct reprogramming of fibroblasts into functional cardiomyocytes by defined factors. Cell. 2010;142:375–86.
39. Tsuji H, Miyoshi S, Ikegami Y, Hida N, Asada H, Togashi I, Suzuki J, Satake M, Nakamizo H, Tanaka M, Mori T, Segawa K, Nishiyama N, Inoue J, Makino H, Miyado K, Ogawa S, Yoshimura Y, Umezawa A. Xenografted human amniotic membrane-derived mesenchymal stem cells are immunologically tolerated and transdifferentiated into cardiomyocytes. Circ Res. 2010;106:1613–23.
40. Bergmann O, Bhardwaj RD, Bernard S, Zdunek S, Barnabe-Heider F, Walsh S, Zupicich J, Alkass K, Buchholz BA, Druid H, Jovinge S, Frisen J. Evidence for cardiomyocyte renewal in humanso. Science. 2009;324:98–102.
41. Messina E, De Angelis L, Frati G, Morrone S, Chimenti S, Fiordaliso F, Salio M, Battaglia M, Latronico MV, Coletta M, Vivarelli E, Frati L, Cossu G, Giacomello A. Isolation and expansion of adult cardiac stem cells from human and murine heart. Circ Res. 2004;95:911–21.
42. Beltrami AP, Barlucchi L, Torella D, Baker M, Limana F, Chimenti S, Kasahara H, Rota M, Musso E, Urbanek K, Leri A, Kajstura J, Nadal-Ginard B, Anversa P. Adult cardiac stem cells are multipotent and support myocardial regeneration. Cell. 2003;114:763–76.
43. Matsuura K, Nagai T, Nishigaki N, Oyama T, Nishi J, Wada H, Sano M, Toko H, Akazawa H, Sato T, Nakaya H, Kasanuki H, Komuro I. Adult cardiac Sca-1-positive cells differentiate into beating cardiomyocytes. J Biol Chem. 2004;279:11384–91.
44. Martin CM, Meeson AP, Robertson SM, Hawke TJ, Richardson JA, Bates S, Goetsch SC, Gallardo TD, Garry DJ. Persistent expression of the ATP-binding cassette transporter, Abcg2, identifies cardiac SP cells in the developing and adult heart. Dev Biol. 2004;265:262–75.
45. Tateishi K, Ashihara E, Takehara N, Nomura T, Honsho S, Nakagami T, Morikawa S, Takahashi T, Ueyama T, Matsubara H, Oh H. Clonally amplified cardiac stem cells are regulated by Sca-1 signaling for efficient cardiovascular regeneration. J Cell Sci. 2007;120:1791–800.
46. Takehara N, Tsutsumi Y, Tateishi K, Ogata T, Tanaka H, Ueyama T, Takahashi T, Takamatsu T, Fukushima M, Komeda M, Yamagishi M, Yaku H, Tabata Y, Matsubara H, Oh H. Controlled delivery of basic fibroblast growth factor promotes human cardiosphere-derived cell engraftment to enhance cardiac repair for chronic myocardial infarction. J Am Coll Cardiol. 2008;52:1858–65.

J Artif Organs (2011) 14:215–222
DOI 10.1007/s10047-011-0568-6

ORIGINAL ARTICLE

Efficient transfection method using deacylated polyethylenimine-coated magnetic nanoparticles

Daisuke Kami · Shogo Takeda · Hatsune Makino · Masashi Toyoda · Yoko Itakura · Satoshi Gojo · Shunei Kyo · Akihiro Umezawa · Masatoshi Watanabe

Received: 6 October 2010 / Accepted: 31 March 2011 / Published online: 3 May 2011

Abstract Low efficiencies of nonviral gene vectors, such as transfection reagent, limit their utility in gene therapy. To overcome this disadvantage, we report on the preparation and properties of magnetic nanoparticles [diameter (d) = 121.32 ± 27.36 nm] positively charged by cationic polymer deacylated polyethylenimine (PEI max), which boosts gene delivery efficiency compare with polyethylenimine (PEI), and their use for the forced expression of plasmid delivery by application of a magnetic field. Magnetic nanoparticles were coated with PEI max, which enabled their electrostatic interaction with negatively charged molecules such as plasmid. We successfully transfected 81.1 ± 4.0% of the cells using PEI max-coated magnetic nanoparticles (PEI max-nanoparticles). Along with their superior properties as a DNA delivery vehicle, PEI max-nanoparticles offer to deliver various DNA formulations in addition to traditional methods. Furthermore, efficiency of the gene transfer was not inhibited in the presence of serum in the cells. PEI max-nanoparticles may be a promising gene carrier that has high transfection efficiency as well as low cytotoxicity.

Keywords Deacylated polyethylenimine · Magnetic nanoparticle · Efficient nonviral transfection method

D. Kami
Innovative Integration between Medicine and Engineering Based on Information Communications Technology, Yokohama National University Global COE Program, Yokohama, Japan
e-mail: dkami@tmig.or.jp

S. Takeda · M. Watanabe (✉)
Laboratory for Medical Engineering, Division of Materials and Chemical Engineering, Yokohama National University, 79-1 Tokiwadai, Hodogaya-ku, Yokohama 240-8501, Japan
e-mail: mawata@ynu.ac.jp

D. Kami · H. Makino · M. Toyoda · A. Umezawa
Department of Reproductive Biology, National Institute for Child Health and Development, Tokyo, Japan

D. Kami · M. Toyoda (✉) · Y. Itakura · S. Gojo
Vascular Medicine, Research Team for Geriatric Medicine, Tokyo Metropolitan Institute of Gerontology, 35-2 Sakae-cho, Itabashi-ku, Tokyo 173-0015, Japan
e-mail: mtoyoda@tmig.or.jp

S. Gojo · S. Kyo
Division of Therapeutic Strategy for Heart Failure, Department of Cardio-Thoracic Surgery, The University of Tokyo, Tokyo, Japan

Introduction

Nanotechnologies that allow the nondisruptive introduction of carriers in vivo have wide potential for gene and therapeutic delivery systems [1–4]. Extremely small particles have been successfully introduced into living cells without any further modification to enhance endocytic internalization, such as for cationic help. The cells containing the internalized nanoparticles continued to thrive, indicating that the particles have no inhibitory effect on mitosis. Therefore, iron oxide magnetic nanoparticles have played an important role as magnetic resonance imaging contrast agents [5, 6], and cytotoxicity of this nanoparticle was none (or low) [7, 8]. Thereby, the functionalized iron oxide magnetic nanoparticles are expected to be useful as a new gene delivery tool [3].

Cationic polymer polyethylenimine (PEI) (linear, MW 25,000) is known as the transfection reagent in molecular biology [9], and the dispersant in nanotechnology [10]. PEI are configured to form the positively charged complex with DNA, which binds to anionic cell surface residues and

enter the cell via endocytosis [9, 11], keeping the dispersed state in the solution [10]. However, PEI containing residual *N*-acyl groups is a disadvantage for transfection efficiency. Also, the deacylated PEI (PEI max) for transfection reagent was reported, showing an increase in optimal transfection efficiency of 21-fold in comparison with PEI [12].

The transfection method using magnetic nanoparticles utilizes a magnetic force to deliver DNA into target cells. Therefore, the plasmid is first associated with magnetic nanoparticles. Then, the application of a magnetic force drives the plasmid–nanoparticle complexes toward and into the target cells, where the cargo is released (Fig. 1a) [13–16]. The magnetic nanoparticles are also coated with biological polymers, such as PEI, to allow plasmid loading (Fig. 1b). The binding of the negatively charged plasmid to the positively charged PEI max-coated magnetic nanoparticles (PEI max-nanoparticles) occurs relatively quickly. After complex formation, the loaded nanoparticles are incubated together with the target cells on a magnet plate. Owing to the magnetic force, the iron particles are rapidly drawn toward the surface of the cell membrane. Cellular uptake occurs by either endocytosis or pinocytosis [17]. Once delivered to the target cells, the plasmid is released into the cytoplasm [17, 18]. The magnetic nanoparticles accumulate in endosomes and/or vacuoles [18]. Over time, the nanoparticles are degraded and the iron enters normal iron metabolism [19]. An influence of magnetic nanoparticles on cellular functions has not been reported yet. However, in most cases, the increased iron concentration in culture media does not lead to cytotoxic effects [7].

In this study, we coated the transfection reagent, PEI max, on the surface of magnetic nanoparticles and applied a gene vector using PEI max-nanoparticles for a highly efficient transfection method. Our results indicate a high level of expression of the transfected gene in living cells using the plasmid-conjugated PEI max-nanoparticles.

Materials and methods

Materials

Magnetic nanoparticles (γ-Fe_2O_3, $d = 70$ nm) were purchased from CIK NanoTek. PEI max linear (MW 25,000) was purchased from Polysciences Inc. FuGENE HD was purchased from Roche Diagnostics. Deionized water was purchased from Gibco. Magnetic sheet (160 mT), and neodymium magnet (130 mT) was purchased from Magna Co. Ltd.

Preparation of the PEI max-nanoparticles

The magnetic nanoparticles (1.0 g) were dissolved in 30 ml of PEI max solution (1.6 mg PEI max/ml). The mixture was sonicated for 2 min (40 W) on ice, and 20 ml of deionized water was added (final concentration 1.0 mg PEI max/ml). The ferrofluid was centrifuged at 4,100×*g* for 5 min. The supernatant fluids were harvested and transferred into a fresh tube. This fluid was washed twice by deionized water and resolved into an equal volume of the PEI max solution (1.0 mg PEI max/ml). Magnetic nanoparticles in this fluid

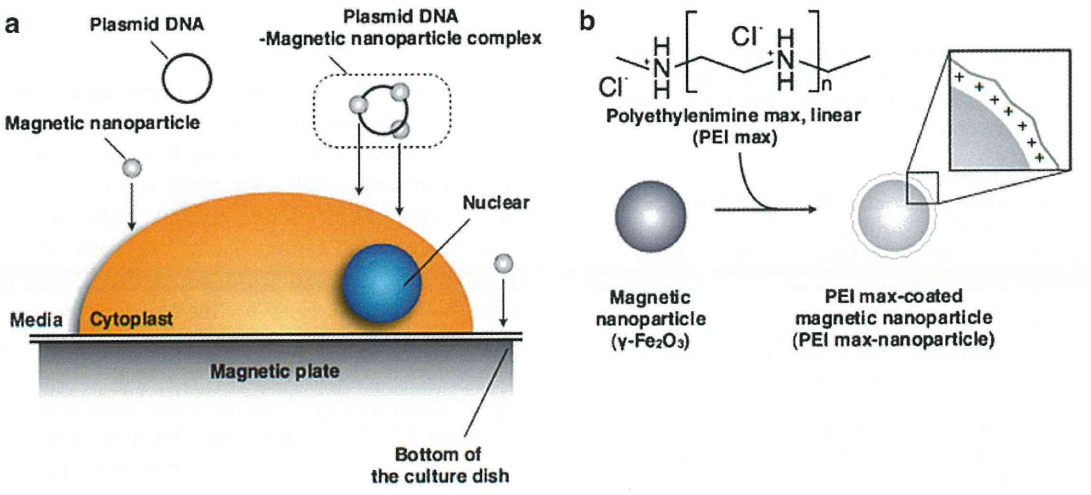

Fig. 1 Nanoparticle transfection method and cationic coating: **a** Plasmid-conjugated magnetic nanoparticles moved to the cell surface on the magnetic sheet upon application of magnetic force. Then, the magnetic force drove this complex toward and into the target cells. **b** Magnetic nanoparticles (γ-Fe_2O_3, $d = 70$ nm) (CIK NanoTek Inc.) were coated with deacylated polyethylenimine max linear (PEI max) (MW 25,000) (Polysciences Inc.), known as a dispersive agent, and transfection reagents. The surface of the PEI max-nanoparticle was positively charged. Nanoparticles and plasmid formed complexes by ionic interaction of the negatively charged plasmid and the positively charged surface of the PEI max-nanoparticle

were coated with PEI max and dispersed in PEI max solution or deionized water.

Measurement of PEI max-nanoparticle size and ζ-potential

The size of the PEI max-nanoparticles was measured with a laser light-scattering method using a fiberoptics particle analyzer (FPAR-1000, Otsuka Electronics). The measurement was performed in triplicate, and median size and range of size distribution were obtained. The ζ-potential of the PEI max-nanoparticles was determined with electrophoretic light-scattering spectrophotometer (ELSZ-2, Otsuka Electronics).

Charge characteristics of PEI max-nanoparticle

PEI max-nanoparticle (100 μg) and each weight of plasmid (2,000, 1,000, 750, 500, 375, 250, 188 ng) were mixed in deionized water or PEI max solution (1 mg/ml). Each solution were reacted for 1 h at room temperature.

Plasmid DNA was bound to PEI max-nanoparticles

Plasmid DNA (5 μg) was reacted with various weights of PEI max-nanoparticles (0–1.8 mg/tube) in deionized water for 15 min at room temperature. Then, the reaction mixtures were centrifuged at 12,000×*g* for 15 min and were formed in a sol-like precipitation in the lower layer. The concentration of DNA in the upper layer (hyaline layer) was determined by NanoDrop 1000 spectrophotometer (Thermo Scientific). The relative concentration of plasmid DNA treated without PEI max-nanoparticles was regarded as 100%.

Cell culture

P19CL6 cells (CL6 cells) from a mouse embryonic carcinoma cell line were grown on 100-mm dishes (Becton-Dickinson) in alpha-minimum essentioal medium (MEM) (Nacalai Tesque) supplemented with 10% fetal bovine serum (FBS) (JRH Bioscience Inc.), penicillin, and streptomycin (Gibco), and were maintained in a 5% carbon dioxide (CO_2) atmosphere at 37°C.

Transfection procedure using PEI max-nanoparticles

CL6 cells were seeded at 1×10^5 cells/well in six-well plates (Becton-Dickinson) 18 h before transfection. Immediately before transfection, cells were rinsed and supplemented with fresh culture medium (1 ml). The PEI max-nanoparticles (in 1 mg PEI max/ml solution) were mixed with 2.0 μg of the plasmid [pCAGGS–enhanced green fluorescent protein (EGFP), the modified pCAGGS expression vector [20], weight ratio PEI max:plasmid = 3:1] and incubated in the deionized water at final volume of 50 μl at room temperature for 15 min. The complexes were added to the CL6 cells on a magnetic sheet various times (0, 0.5, 1, 4, and 24 h). Forty-eight hours after transfection, CL6 cells were evaluated; 1 mg/ml of PEI max solution was used as a positive control.

Quantitative real-time reverse transcriptional (RT)-PCR

Total RNAs from CL6 cells were extracted using ISOGEN (Nippon Gene). To perform quantitative real-time polymerase chain reaction (PCR) assay, total RNA (1 μg) was reverse-transcribed using random hexamer and the PrimeScript RT reagent kit (TaKaRa). Quantitative real-time reverse transcriptional (RT)-PCR was performed on LineGene (BioFlux), using 100 ng of complementary DNA (cDNA) in 25 μl reaction volumes with 10 nmol/l EGFP primer and 12.5 μl of SYBR Premix Ex Taq (TaKaRa). PCR primers for the gene of EGFP and *Gapdh* were designed to amplify each cDNA using the sense primer (5′-CCGACCACATGAAGCAGCAC-3′) and the reverse primer (5′-CTTCAGCTCGATGCGGTTCAC-3′) for the EGFP, and the sense primer (5′-TGCGACTTCAACAGCA ACTC-3′) and the reverse primer (5′-CTTGCTCAGTGTC CTTGCTG-3′) for the *Gapdh*. Calculations were automatically performed by fluorescent quantitative detection system software (BioFlux).

Nanoparticle cytotoxicity

Alamar Blue [21] was used to measure cell proliferation and metabolic activity as an oxidation-reduction indicator. After 48 h of PEI max or PEI max-nanoparticle exposure, 900 μl of medium from each condition was transferred into a 24-well flat-bottomed plate. One hundred microliters of Alamar Blue (AbD Serotec) was added to each well, and the well plate was incubated for 3 h at 37°C. Fluorescence was measured at 570/600 nm in a Viento multispectrophotometer reader (Dainippon Pharmaceutical). The relative absorbance of CL6 cells without any treatment is regarded as 100% (it is indicated as a percent control in Fig. 4c).

Flow cytometric analysis

To count the numbers of EGFP-positive cells using PEI max-nanoparticles (0.8 μg/well in a six-well plate) on a magnetic sheet for 4 h (PEI max alone as a positive control), a Cytomics FC500 (Beckman Coulter Inc.) was used, and data were analyzed with FlowJo Ver.7 (Tree Star Inc.). Each sample was compared with negative control cells (without treatment).

Statistical analysis

Results, shown as the mean ± standard error (SE), were compared by analysis of variance (ANOVA) followed by Scheffe test (http://chiryo.phar.nagoya-cu.ac.jp/javastat/JavaStat-j.htm), with $P < 0.05$ considered significant.

Results

Characterization of PEI max-nanoparticles

Magnetic nanoparticles were well coated with PEI max and were highly dispersed in PEI max solution (1 mg/ml) or deionized water. Secondary size of the PEI max-nanoparticles was approximately 121.32 ± 27.36 nm (Fig. 2A). To evaluate stability in PEI max solution (1 mg/ml) or deionized water, we measured the ζ-potential of PEI max-nanoparticles, which was +45.53 mV in PEI max solution and +30.05 mV in deionized water. The PEI max-nanoparticles were aggregated by magnetic force (Fig. 2Ba) and quickly redispersed by vortex (Fig. 2Bb). Time-lapse photography (30 s/s) shows that magnetic nanoparticles were gradually removed at the site of the neodymium magnet (right side of the tube) for 2 h (magnetic nanoparticles for transfection: http://www.youtube.com/watch?v=Hyjfc4moHK4). These nanoparticles in PEI max solution were not aggregated without magnetic force. To avoid aggregation of plasmid-attached PEI max-nanoparticle caused by charge neutralization, it was necessary that their weight ratio was approximately 1:400 (Fig. 2C). In general, 1–2 μg of plasmid per well was mixed with the transfection reagent such, as PEI max, and FuGENE HD into six-well plates. However, too much (400–800 μg of nanoparticle per well) caused inhibition of transfection (described later). To solve the problem, we decided to use in 1 mg/ml of PEI max solution as a solvent. As a result, each concentration of the plasmid did not aggregate with PEI max-nanoparticle (Fig. 2Bb). To evaluate whether the plasmid DNA was attached to PEI max-nanoparticles in deionized water, we reacted PEI max-nanoparticles with plasmid DNA for 15 min at room temperature. Measuring the concentration of plasmid DNA in the upper layer (hyaline layer), the weight of PEI max-nanoparticles was reduced in a dependent manner (Fig. 2D).

Transfection efficiency using PEI max-nanoparticles and magnetic sheet, and viability of the CL6 cells treated with PEI max-nanoparticles

CL6 cells were transfected with pCAGGS-EGFP and PEI max alone as a positive control (Fig. 3a) and pCAGGS-EGFP and PEI max-nanoparticles (Fig. 3b) at 48 h after transfection. Many EGFP-positive cells were observed among CL6 cells transfected with PEI max-nanoparticles compared with those transfected with PEI max. To evaluate the optimum condition of transfection using PEI max-nanoparticles, quantitative real-time RT-PCR was performed at 48 h after transfection. The optimum condition of transfection was a concentration of 0.8 μg/well (Fig. 4a) on a magnetic sheet for 4 h (Fig. 4b). *EGFP* gene expression level was reduced under transfection of excess magnetic nanoparticles (7.5 μg/well) (Fig. 4a) and prolonged time on the magnetic sheet (24 h) (Fig. 4b). EGFP expression in CL6 cells transfected with PEI max-nanoparticles was increased approximately two to fourfold compared with those transfected with PEI max. The viability of CL6 cells treated with PEI max-nanoparticles, as measured by Alamar Blue assay, did not differ between cells treated with/without PEI max alone (Fig. 4c).

Number of EGFP-positive cells by flow cytometric analysis

Forty-eight hours after transfection using PEI max alone or PEI max-nanoparticles, we examined the number of EGFP-positive cells (total 10,000 cells) by flow cytometric analysis. Compared with the negative control (untreated CL6 cells), 42.2 ± 8.5% of cells treated with PEI max alone (Fig. 5a), 81.1 ± 4.0% of cells treated with 0.8 μg of PEI max-nanoparticles per well on the magnetic sheet for 4 h (Fig. 5b), and 13.9 ± 1.1% of cells treated with FuGENE HD (Fig. 5c) expressed EGFP. The number of EGFP-positive cells was significantly increased (approximately twofold) using PEI max-nanoparticles.

Discussion

In this study, to express target gene with high efficiency and low cytotoxicity, we focused on PEI max and magnetic nanoparticles (γ-Fe_2O_3). Many researchers have reported various transfection methods using PEI and magnetic nanoparticles, such as γ-Fe_2O_3, and superparamagnetic iron oxide nanoparticle (used as magnetic resonance imaging contrast agents) (Table 1). However, these methods had a low transfection efficiency [14, 15], combined with virus (adenovirus, or retrovirus) [15], and high cytotoxicity (low cell viability) [13] and may therefore have little effectiveness for clinical use.

The expression level of the *EGFP* gene was reduced under transfection of excess magnetic nanoparticles (7.5 μg/well) (Fig. 4a). This result may indicate that a high concentration of PEI max-nanoparticles formed the large agglutinate complexes with plasmid DNAs [22, 23]

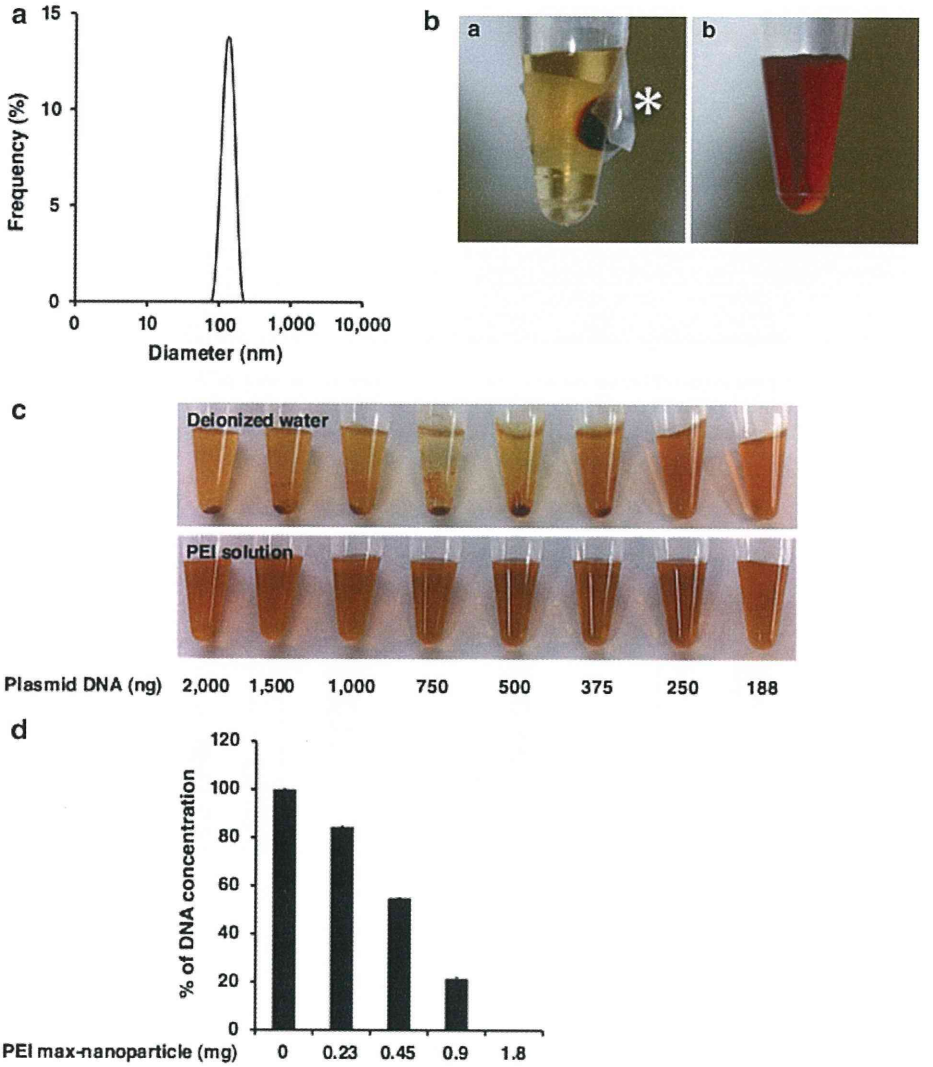

Fig. 2 Characteristics of the deacylated polyethylenimine (PEI max)-nanoparticle: **a** The size of the PEI max-nanoparticles was measured with a laser light-scattering method using a fiberoptics particle analyzer (FPAR-1000, Otsuka Electronics) at 37°C. Secondary particle size of the PEI max-nanoparticles was approximately 121.32 ± 27.36 nm. **b** PEI max-nanoparticles were induced to aggregate by a magnet (*a*) and were then dispersed (*b*). *Asterisk* indicates column-shaped neodymium magnet. **c** Cationic PEI max-nanoparticles (100 μg per tube) in deionized water or PEI max solution (1 mg/ml) were reacted with anionic plasmid [pCAGGS–enhanced green fluorescent protein (EGFP)] by an ionic bond. PEI max-nanoparticles in deionized water and plasmid aggregated more easily than that in PEI max solution and plasmid. **d** To evaluate whether plasmid DNA attached to PEI max-nanoparticles in deionized water, PEI max-nanoparticles were reacted with plasmid DNA for 15 min at room temperature. Measuring the concentration of plasmid DNA in the upper layer (hyaline layer), the weight of PEI max-nanoparticles was reduced in a dependent manner

because PEI max-nanoparticle and plasmid DNA complexes are taken in by endocytosis. Thus, it might be difficult to take the large complexes into the cytoplasm by endocytosis. Furthermore, the expression level of the *EGFP* gene was also reduced under transfection during a prolonged time on the magnetic sheet (24 h) (Fig. 4b). This result may demonstrate a causal relationship between the cell division cycle and time on the magnetic sheet. Plasmid DNAs in the cytoplasm were transported into the nucleus when the nuclear membrane disappeared on cell division [24]. Thus, plasmid DNAs and magnetic nanoparticle complexes might not be transported into the nucleus because they are drawn to the bottom of the cell by magnetic force.

We succeeded in producing PEI max-nanoparticles that enabled P19CL6 cells, which is derived from embryonic carcinoma transfected on a magnetic sheet. In addition, this method resulted in a highly efficient gene transduction compared with that of conventional transfection methods (Fig. 5a, c). This transfection method using PEI max-nanoparticles is a relatively low-cost and quick method of

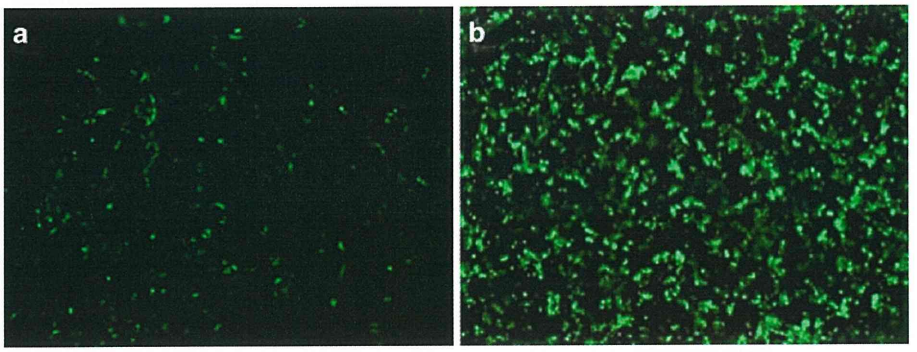

Fig. 3 Enhanced green fluorescent protein (EGFP) expression in CL6 cells using deacylated polyethylenimine (PEI max)-nanoparticle and magnetic field. Phase-contrast fluorescent micrograph of CL6 cells were transfected with pCAGGS-EGFP and PEI max as a control (**a**) and PEI max-nanoparticles (**b**). The numbers of EGFP-positive cells were further increased by PEI max-nanoparticles

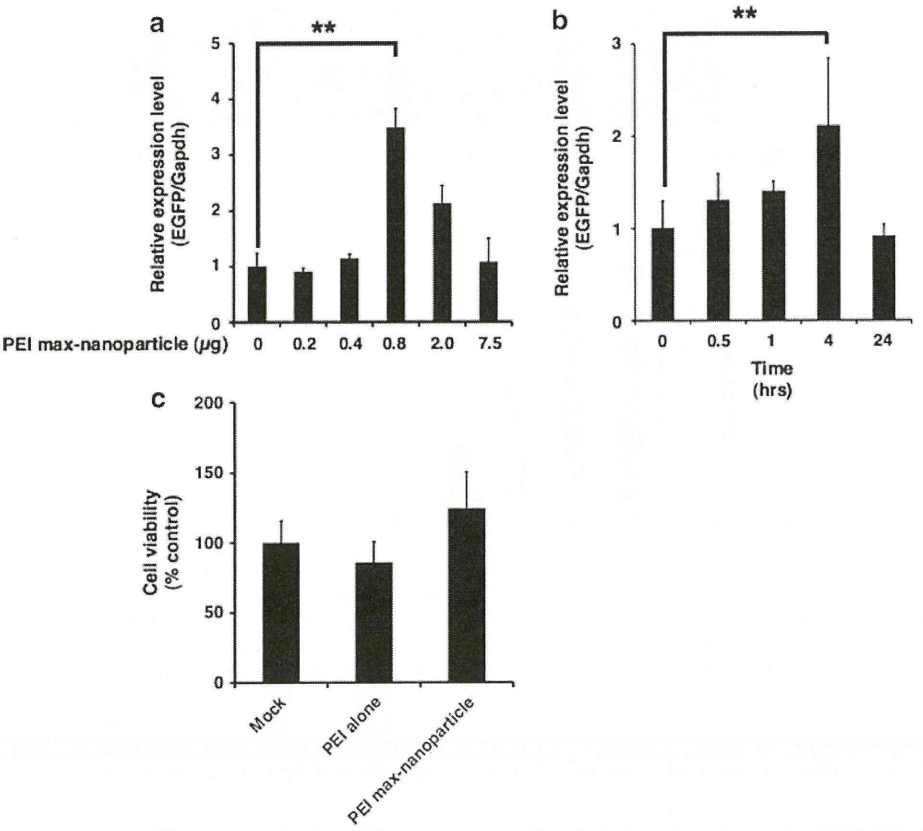

Fig. 4 Optimum condition for transfection of the deacylated polyethylenimine (PEI max)-nanoparticle. To optimize the transfection method, we examined PEI max-nanoparticles in terms of volume (**a**) and time (**b**) on the magnetic sheet. These results were evaluated by quantitative real-time reverse transcriptional polymerase chain reaction (RT-PCR). The expression level of the CL6 cells treated with PEI max alone is regarded as 1. The optimal conditions for transfection using PEI max-nanoparticles were when the CL6 cells were treated with 0.8 μg of PEI max-nanoparticles and 2.0 μg of pCAGGS-EGFP for 4 h on the magnetic sheet. The *double asterisks* indicate a significant difference ($P < 0.05$). Cytotoxicities of PEI max and PEI max-nanoparticles were evaluated by Alamar Blue assay (**c**). After 48 h of PEI max or PEI max-nanoparticle exposure, there were no significant differences in cell viability between CL6 cells treated with PEI max and those with PEI max-nanoparticles. *Mock* the CL6 cells treated without any treatment as a negative control. *PEI max alone* the CL6 cells treated with PEI max. *PEI max-nanoparticles* the CL6 cells treated with PEI max-nanoparticles (0.8 μg) for 4 h on the magnetic sheet. The relative absorbance of untreated CL6 cells is regarded as 100%

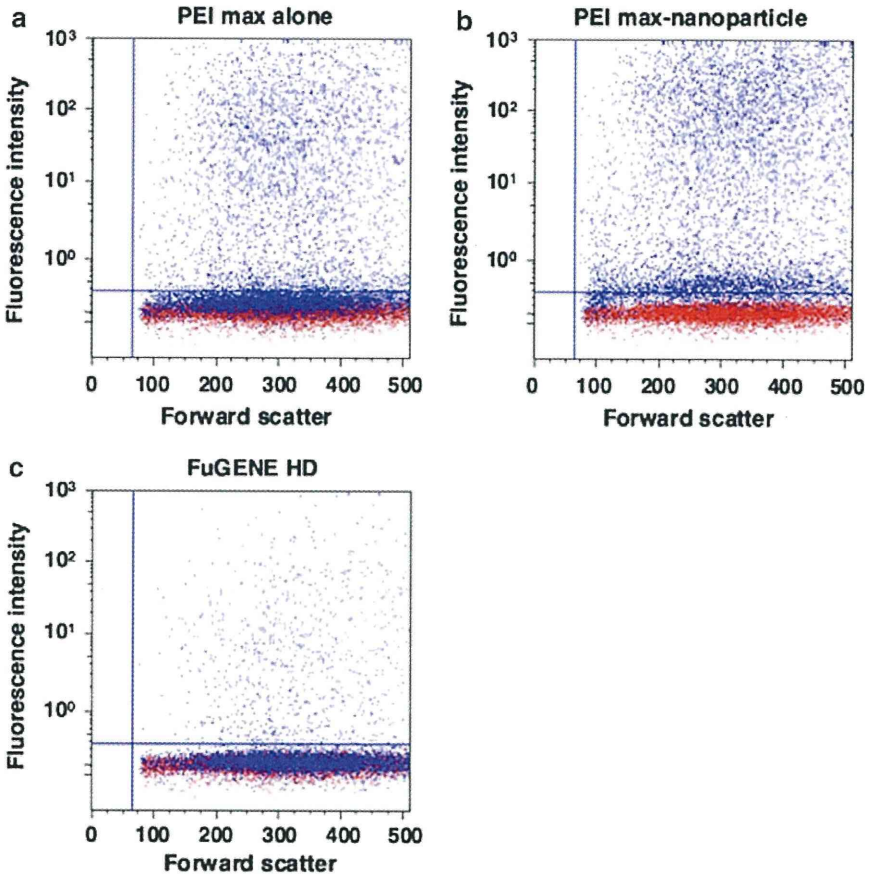

Fig. 5 Transfection efficiency of the deacylated polyethylenimine (PEI max)-nanoparticle. Comparison of scattering properties of the untreated CL6 cells (mock, *red dot*) and with PEI max alone (**a**, *blue dot*, 42.2 ± 8.5%), PEI max-nanoparticles (**b**, *blue dot*, 81.1 ± 4.0%), or FuGENE HD (**c**, *blue dot*, 13.9 ± 1.1%) by flow cytometry

Table 1 Comparison of transfection methods using the polyethylenimine and magnetic nanoparticles

Author	Year	Vector	Component	Cell	Transfection efficiency	Cell viability (% of control)	References
Kami	–	Plasmid	PEI max (MW 25k), MNP (γ-Fe2O3, 70 nm), MF (0.2 T)	P19CL6	80%[a]	100	This paper
Zhang	2010	Plasmid	Branched PEI (MW 25k), SPION (30 nm), MF (1.2 T)	NIH3T3	64%[a]	100	[14]
		siRNA	Branched PEI (MW 25k), SPION (30 nm), MF (1.2 T)	NIH3T3	77%[a]	100	
Kievit	2009	Plasmid	PEI (MW 25k), SPION (200 nm)	C6	90%[a]	10	[13]
		Plasmid	PEI (MW 25k), Chitosan, SPION (200 nm)	C6	45%[a]	100	
		Plasmid	PolyMag (commercial magnification reagent), MF (1.2 T)	C6	32%[a]	66	
Scherer	2002	Plasmid	PEI (MW 800k), SPION (200 nm), MF (1 T)	NIH3T3	5-fold[b]	–	[15]
		Adenovirus	PEI (MW 800k), SPION (200 nm), MF (1 T)	K562	100-fold[b]	–	
		Retrovirus	PEI (MW 800k), SPION (200 nm), MF (1 T)	NIH3T3	20%[a]	–	

Transfection efficiency indicates optimal transfection condition

PEI polyethylenimine, *PEI max* deacylated PEI, *MNP* magnetic nanoparticle, *SPION* superparamagnetic iron oxide nanoparticle, *MW* molecular weight, *MF* magnetic force, *T* tesla

[a] Flowcytometric analysis

[b] Luciferase activity assay

introducing plasmid into target cells with increased efficiency. Furthermore, a major advantage of this method is its tolerability among cells. Other methods might be limited either by possible cytotoxic effects of the lipidic transfection reagent (lipofection) or simply by the directly applied force on the cells (electroporation). In contrast, methods such as lipofection offer only a certain probability of hits between cargo and cells because of the three-dimensional motion of cells and transfection aggregates in a liquid suspension. Normally, transfection was inhibited

by serum using transfection reagent [25]. However, this method can also be performed in the presence of serum, which is a further benefit. Additionally, synergistic effects on transfection efficiency can arise from the possible combination of PEI max and nanoparticles. This technology might be an alternative to the currently used viral and nonviral vectors in gene therapy and gene transfer [26].

Our results suggest that PEI max-nanoparticles offer the ability to deliver various DNA formulations in addition to the traditional methods. Furthermore, gene transfer efficiency was not inhibited in the presence of serum in the cells. PEI max-nanoparticles may be a promising gene carrier with high transfection efficiency and low cytotoxicity.

Acknowledgments We express our sincere thanks to Koichiro Nishino (Department of Reproductive Biology, National Institute for Child Health and Development) for pCAGGS-EGFP. This study was supported by a Grant-in-Aid for the Global COE Program, Science for Future Molecular Systems from the Ministry of Education, Culture, Sports, Science and Technology, Japan (MEXT).

References

1. Kimura T, Iwai S, Moritan T, Nam K, Mutsuo S, Yoshizawa H, Okada M, Furuzono T, Fujisato T, Kishida A. Preparation of poly(vinyl alcohol)/DNA hydrogels via hydrogen bonds formed on ultra-high pressurization and controlled release of DNA from the hydrogels for gene delivery. J Artif Organs. 2007;10:104–8.
2. Moritake S, Taira S, Ichiyanagi Y, Morone N, Song SY, Hatanaka T, Yuasa S, Setou M. Functionalized nano-magnetic particles for an in vivo delivery system. J Nanosci Nanotechnol. 2007;7:937–44.
3. Tomitaka A, Koshi T, Hatsugai S, Yamada T, Takemura Y. Magnetic characterization of surface-coated magnetic nanoparticles for biomedical application. J Magn Magn Mater. 2010;323: 1396–1403.
4. Yokoyama M. Drug targeting with nano-sized carrier systems. J Artif Organs. 2005;8:77–84.
5. Lauterbur PC, et al. Image formation by induced local interactions. Examples employing nuclear magnetic resonance. Clin Orthop Relat Res. 1973;1989:3–6.
6. Nakamura H, Ito N, Kotake F, Mizokami Y, Matsuoka T. Tumor-detecting capacity and clinical usefulness of SPIO-MRI in patients with hepatocellular carcinoma. J Gastroenterol. 2000;35: 849–55.
7. Karlsson HL, Cronholm P, Gustafsson J, Moller L. Copper oxide nanoparticles are highly toxic: a comparison between metal oxide nanoparticles and carbon nanotubes. Chem Res Toxicol. 2008; 21:1726–32.
8. Karlsson HL, Gustafsson J, Cronholm P, Moller L. Size-dependent toxicity of metal oxide particles–a comparison between nano- and micrometer size. Toxicol Lett. 2009;188:112–8.
9. Boussif O, Lezoualc'h F, Zanta MA, Mergny MD, Scherman D, Demeneix B, Behr JP. A versatile vector for gene and oligonucleotide transfer into cells in culture and in vivo: polyethylenimine. Proc Natl Acad Sci USA. 1995;92:7297–301.
10. Wang J, Gao L. Adsorption of polyethylenimine on nanosized zirconia particles in aqueous suspensions. J Colloid Interface Sci. 1999;216:436–9.
11. Vancha AR, Govindaraju S, Parsa KV, Jasti M, Gonzalez-Garcia M, Ballestero RP. Use of polyethyleneimine polymer in cell culture as attachment factor and lipofection enhancer. BMC Biotechnol. 2004;4:23.
12. Thomas M, Lu JJ, Ge Q, Zhang C, Chen J, Klibanov AM. Full deacylation of polyethylenimine dramatically boosts its gene delivery efficiency and specificity to mouse lung. Proc Natl Acad Sci USA. 2005;102:5679–84.
13. Kievit FM, Veiseh O, Bhattarai N, Fang C, Gunn JW, Lee D, Ellenbogen RG, Olson JM, Zhang M. PEI-PEG-chitosan copolymer coated iron oxide nanoparticles for safe gene delivery: synthesis, complexation, and transfection. Adv Funct Mater. 2009;19:2244–51.
14. Zhang H, Lee MY, Hogg MG, Dordick JS, Sharfstein ST. Gene delivery in three-dimensional cell cultures by superparamagnetic nanoparticles. ACS Nano. 2010;4:4733–43.
15. Scherer F, Anton M, Schillinger U, Henke J, Bergemann C, Kruger A, Gansbacher B, Plank C. Magnetofection: enhancing and targeting gene delivery by magnetic force in vitro and in vivo. Gene Ther. 2002;9:102–9.
16. Bertram J. MATra—magnet assisted transfection: combining nanotechnology and magnetic forces to improve intracellular delivery of nucleic acids. Curr Pharm Biotechnol. 2006;7: 277–85.
17. Arsianti M, Lim M, Marquis CP, Amal R. Polyethylenimine based magnetic iron-oxide vector: the effect of vector component assembly on cellular entry mechanism, intracellular localization, and cellular viability. Biomacromolecules. 2010;11:2521–31.
18. Georgieva JV, Kalicharan D, Couraud PO, Romero IA, Weksler B, Hoekstra D, Zuhorn IS. Surface characteristics of nanoparticles determine their intracellular fate in and processing by human blood-brain barrier endothelial cells in vitro. Mol Ther. 2011; 19:318–25.
19. Longmire M, Choyke PL, Kobayashi H. Clearance properties of nano-sized particles and molecules as imaging agents: considerations and caveats. Nanomedicine (Lond). 2008;3:703–17.
20. Niwa H, Yamamura K, Miyazaki J. Efficient selection for high-expression transfectants with a novel eukaryotic vector. Gene. 1991;108:193–9.
21. Nakayama GR, Caton MC, Nova MP, Parandoosh Z. Assessment of the Alamar blue assay for cellular growth and viability in vitro. J Immunol Methods. 1997;204:205–8.
22. Namgung R, Singha K, Yu MK, Jon S, Kim YS, Ahn Y, Park IK, Kim WJ. Hybrid superparamagnetic iron oxide nanoparticle-branched polyethylenimine magnetoplexes for gene transfection of vascular endothelial cells. Biomaterials. 2010;31:4204–13.
23. Song HP, Yang JY, Lo SL, Wang Y, Fan WM, Tang XS, Xue JM, Wang S. Gene transfer using self-assembled ternary complexes of cationic magnetic nanoparticles, plasmid DNA and cell-penetrating Tat peptide. Biomaterials. 2010;31:769–78.
24. Coonrod A, Li FQ, Horwitz M. On the mechanism of DNA transfection: efficient gene transfer without viruses. Gene Ther. 1997;4:1313–21.
25. Purow BW, Sundaresan TK, Burdick MJ, Kefas BA, Comeau LD, Hawkinson MP, Su Q, Kotliarov Y, Lee J, Zhang W, Fine HA. Notch-1 regulates transcription of the epidermal growth factor receptor through p53. Carcinogenesis. 2008;29:918–25.
26. Davis ME. Non-viral gene delivery systems. Curr Opin Biotechnol. 2002;13:128–31.

Int. J. Mol. Sci. **2011**, *12*, 3705-3722; doi:10.3390/ijms12063705

OPEN ACCESS

International Journal of
Molecular Sciences
ISSN 1422-0067
www.mdpi.com/journal/ijms

Review

Application of Magnetic Nanoparticles to Gene Delivery

Daisuke Kami [1,*], Shogo Takeda [2], Yoko Itakura [1], Satoshi Gojo [1], Masatoshi Watanabe [2] and Masashi Toyoda [1]

[1] Research Team for Vascular Medicine, Tokyo Metropolitan Institute of Gerontology, 35-2 Sakae-cho, Itabashi-ku, Tokyo 173-0015, Japan; E-Mails: yitakura@tmig.or.jp (Y.I.); satoshigojo-tky@umin.ac.jp (S.G.); mtoyoda@tmig.or.jp (M.T.)

[2] Laboratory for Medical Engineering, Division of Materials and Chemical Engineering, Yokohama National University, 79-1 Tokiwadai, Hodogaya-ku, Yokohama 240-8501, Japan; E-Mails: smilesnow1987@gmail.com (S.T.); mawata@ynu.ac.jp (M.W.)

* Author to whom correspondence should be addressed; E-Mail: dkami@tmig.or.jp; Tel.: +81-3-3964-3241; Fax: +81-3-3579-4776.

Received: 6 May 2011; in revised form: 18 May 2011 / Accepted: 25 May 2011 / Published: 7 June 2011

Abstract: Nanoparticle technology is being incorporated into many areas of molecular science and biomedicine. Because nanoparticles are small enough to enter almost all areas of the body, including the circulatory system and cells, they have been and continue to be exploited for basic biomedical research as well as clinical diagnostic and therapeutic applications. For example, nanoparticles hold great promise for enabling gene therapy to reach its full potential by facilitating targeted delivery of DNA into tissues and cells. Substantial progress has been made in binding DNA to nanoparticles and controlling the behavior of these complexes. In this article, we review research on binding DNAs to nanoparticles as well as our latest study on non-viral gene delivery using polyethylenimine-coated magnetic nanoparticles.

Keywords: magnetic nanoparticles; Magnetofection; gene delivery; polyethylenimine

---

1. Introduction

Nanotechnology describes the creation and utilization of materials, devices, and systems through the control of nanometer-sized materials and their application to physics, chemistry, biology, engineering, materials science, medicine, and other endeavors. In particular, intensive efforts are in progress to develop nanomaterials for medical use as agents that can be targeted to specific organs, tissues, and cells. For example, magnetic nanoparticles (MNPs) are being used clinically as contrast agents for magnetic resonance imaging (MRI) (Table 1). MRI is a noninvasive technique that can provide real-time high-resolution soft tissue information [1,2]. MRI image quality can be further improved by utilizing contrast agents that alter proton relaxation rates [3–8]. MNP-based drug delivery systems (DDS) [9–11], and treatments of hyperthermia [12–21], using MNPs have been studied for over a decade. Furthermore, researchers have reported that MNPs have been useful in hyperthermic treatment for various cancers *in vivo* [22–31]. Nanotechnology-based anti-cancer agent DDS have already been approved, such as pegylated liposomal doxorubicin (DOXIL) for ovarian cancer [32–37]. MNPs have been used effectively as transfection reagents for introducing nucleic acids (plasmids or siRNAs) [38–53], or viruses (retrovirus, or adenovirus) [44,54–56] into cells. Our own research is focused on MNP-mediated gene delivery systems (called as "Magnetofection").

Table 1. Biomedical Applications of Magnetic Nanoparticles (MNPs).

	Purpose	References
MRI	Diagnosis	[1–8,57–61]
DDS	Anti-cancer therapy, Enzyme therapy	[9–11,22–31]
Hyperthermia	Anti-cancer therapy	[12–18,33–37]
Gene Delivery	Anti-cancer therapy, Cell transplantation therapy	[38–55]

2. Gene Delivery

Gene delivery techniques efficiently introduce a gene of interest in order to express its encoded protein in a suitable host or host cell. Currently, there are three primary gene delivery systems that employ viral vectors (retroviruses and adenoviruses), nucleic acid electroporation, and nucleic acid transfection. These systems vary in efficacy (Table 2). Gene delivery by viral vectors can be highly efficient (80–90%) but may insert viral vector nucleic acid sequences into the host genome, potentially causing unwelcome effects, such as inappropriate expression of deleterious genes. Electroporation is also a highly efficient technique for introducing foreign genes into a host (50–70%); however, half of the recipient cells die due to the electrical stimulation. Transfection reagents do not efficiently deliver nucleic acids into cells (20–30%); however, cell viability is largely preserved and the method is safe enough for clinical use. Therefore, this method holds relatively more promise for medical applications, provided that its efficiency can be improved. MNPs are already in use by basic researchers to increase transfection efficiencies of cultured cells. Thus, MNP-nucleic acid complexes are added to cell culture media and then onto the cell surface by applying a magnetic force (Figure 1).

Table 2. Gene delivery systems.

	Expression Type	Efficiency (%)	Cell Viability (%)	Safety
Virus *	Stable, or Transient	80–90%	80–90%	Low
Electroporation	Transient	50–70%	40–50%	High
TF reagent **	Transient	20–30%	80–90%	High

* Virus including adenovirus (transient), retrovirus (stable), and lentivirus (stable); ** TF reagent, transfection reagents including PEI (Polysciences Inc.), FuGENE HD (Promega), and Lipofectamine 2000 (Invitrogen); All values are ours (unpublished experiments).

Figure 1. MNP gene delivery system (Magnetofection). Plasmids are bound to MNPs, which then move from the media to the cell surface by applying a magnetic force.

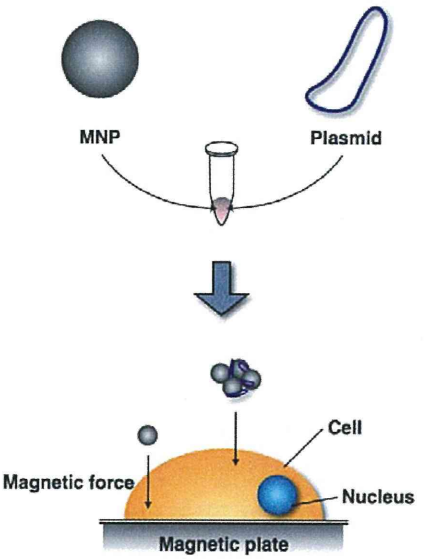

Oxide nanoparticles mixed with high magnetic moment compounds such as $CoFe_2O_4$, $NiFe_2O_4$, and $MnFe_2O_4$ exhibit superior performance compared to other magnetic materials [62,63]. However, these nanoparticles are highly toxic to cells, limiting their use for *in vivo*, and *in vitro* biomedical applications [64–67]. However, iron oxides such as magnetite (Fe_3O_4) and maghemite (γ-Fe_2O_3), in particular, possess high magnetic moments, are relatively safe, and currently in clinical use as MRI contrast agents [57–61]. These iron oxide based-magnetic materials are also suitable for biomedical applications. Fe^{3+} is widely dispersed in the human body so leaching of this metal ion from nanoparticles should not reach toxic concentrations [68,69]. As a result, maghemite is a popular choice for MNPs used biomedical applications. It is very important to modify the surface of MNPs so that they can be used for biomedical applications. Thus, MNPs are coated with compounds such as natural polymers (proteins and carbohydrates) [70–75], synthetic organic polymers (polyethylene glycol), polyvinyl alcohol, poly-L-lactic acid) [72,76–78], silica [79], and gold [80,81]. These surface coating agents prevent nanoparticle agglomeration, cytotoxicity, and add functionality. MNPs agglomerate readily in aqueous solutions around pH 7 [82], and it is difficult to control the properties and amounts of agglomerated MNPs. The greater toxicity of MNPs compared to those of microparticles can be attributed to their high surface to volume ratio [83]. Coating agents prevent the leaching of potentially toxic components from MNPs. In fact, the cytotoxicity of uncoated $NiFeO_4$ MNPs is dramatically

decreased by coating with cationic polymer, polyethylenimine (PEI) [84–86]. PEI, a cationic polymer, is widely used for nucleic acid transfection [87–89] and also serves as a nanoparticle dispersant [90]. PEI-coated MNPs enhance transfection efficiency [38,41,42,44–46,48,49,51,54,55].

3. Cell Transplantation Therapy Using MNPs

Autologous cell transplantation has been widely used in the clinic for decades. Delivering therapeutic genes to patients using their own cells avoids using immunosuppressive drugs. We reasoned, therefore, that a non-viral gene delivery system using iron oxide-based MNPs could provide a powerful tool for next-generation therapies. Gene delivery using MNPs has been successful for delivering nucleic acids into living cells with high efficiency and low cytotoxicity [38,41,42,44–46,48,49,51,54,55]. Currently, there are several methods for inducing cellular differentiation.

One of these methods, termed direct reprogramming, or direct conversion, has successfully yielded induced cardiomyocytes, induced neurons, reprogrammed pancreatic β cells, and induced pluripotent stem cells (iPSCs) [91–95]. Direct reprogramming represents a more straightforward strategy to treat diseases involving loss of function by specific cell populations compared to approaches requiring an intermediate embryonic stem cell. Thus, patient-derived differentiated cells by gene transfer are suitable for autologous cell transplantation, potentially resulting in faster patient recoveries. The scheme is classified into *ex vivo* gene therapy. The steps involved in this technique are as follows: (1) Patient-derived cells (such as fibroblasts) are cultured in chemically defined media *in vitro*; (2) These cells are transfected by MNPs, and differentiated into functional cells; (3) Differentiated cells are isolated by fluorescence-activated cell sorting (FACS); (4) FACS-purified differentiated cells are transplanted into the patient's target tissue (Figure 2).

Here we briefly describe the magnetofection [96], and our latest study concerning non-viral gene delivery using deacylated polyethylenimine coated MNPs.

Figure 2. Strategy for cell transplantation therapy. A patient's cells are cultured in chemically defined media. MNP-transfected cells by the introduced gene are isolated by FACS. FACS-purified differentiated cells are transplanted into the patient.

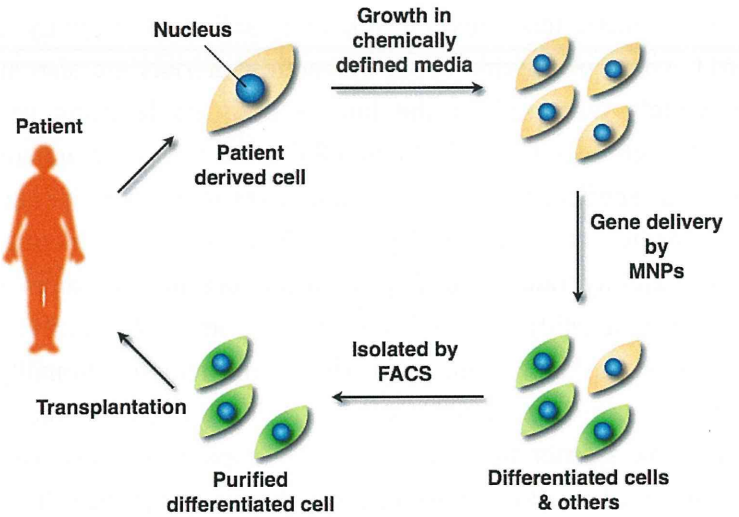

4. Gene Delivery Using MNPs and Magnetic Force

The mechanism of magnetofection is similar to using transfection reagents (Lipofectamine 2000, FuGENE HD, and PEI). The only difference is that the plasmids form complexes with cationic polymer-coated MNPs (called as "Magnetoplex") [42,48,97–99] (Figure 3). Figure 3 shows the two difference techniques. The behavior of magnetoplex is readily controlled by magnetic force. Upon binding to the cell surface they are taken up by endocytosis [51,100,101]. Thus, the transfection efficiency was increased.

Figure 3. Gene delivery systems using a transfection reagent (cationic polymer) and MNPs: (**A**) Gene delivery system using transfection reagent. The polyplex moves randomly in culture medium; (**B**) Magnetofection system. The magnetoplex only moves to the cell surface.

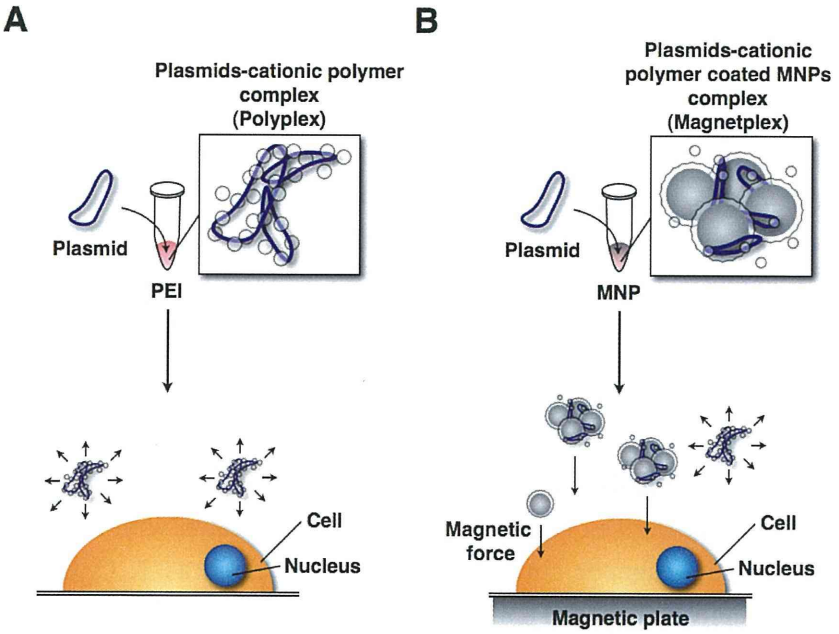

Many researchers have described magnetofection methods (Table 3). They modified the surface of iron oxide-based MNPs to increase transfection efficiency and reduce cytotoxicity. To achieve this, some investigators selected coating agents such as anionic surfactants (oleic acid, lauroyl sarcosinate) [42,50,102], a non-ionic water-soluble surfactant (Pluronic F-127) [42], fluorinated surfactant (lithium 3-[2-(perfluoroalkyl) ethylthio]propionate) [54], a polymer (polyethylene glycol, poly-L-lysine, poly(propyleneimine) dendrimers) [40,103,104], carbohydrates (Chitosan, Heparan sulfate) [41,47], silica particles (MCM48) [49], proteins (serum albumin, streptavidin) [40,55], hydroxyapatite [105], phospholipids [49,50], a cationic cell penetrating peptide (TAT peptide) [43], non-activated virus envelope (HVJ-E) [47], a transfection reagent (Lipofectamine 2000) [53], and viruses (adenovirus, retrovirus) [44,54–56]. These coating agents are often used in conjunction with PEI. PEI is a well-known cationic gene carrier with high transfection efficiency. However, the high toxicity, depended on its molecular weight, has limited its use as a potential gene carrier. Thus, the PEI was modified to increase transfection efficiency, and decrease cytotoxicity [88,106]. To enhance transfection

efficiency, most researchers used the PEI, or the modified PEI to coat the nanoparticle surface [38,41,42,44–46,48,49,51,54,55,102,107]. PEI-coated MNPs are stable in water, bind nucleic acids, and control MNP behavior by magnetic force. In addition, linear PEI possesses low cytotoxicity compared with branched PEI *in vivo* and *in vitro* [108,109] The highest transfection efficiencies have been achieved using 25,000 molecular weight linear PEI [89]. However, PEI cytotoxicity due to its acyl groups has been described [88]. Therefore, our group focused on commercial deacylated PEI (Polyethylenimine "Max" (PEI "Max"), Polysciences Inc.) as an MNP (γ-Fe_2O_3, d = 70 nm, CIK NanoTek) coating agent.

Deacylated polyethylenimine (linear, 25,000 molecular weight) is built from the same polymer backbone as the popular linear polyethylenimine, and possesses high cationic reactivity. PEI "Max"-coated MNPs (PEI max-MNPs) are stable in deionized water, and positively charged. Thus, PEI max-MNPs electrostatically bind to plasmids. We attempted to introduce the green fluorescent protein (GFP) gene into a mouse embryonic carcinoma cell line, P19CL6 using PEI max-MNPs, and succeeded in establishing a highly efficient and low cytotoxic gene delivery system [107]. Furthermore, we applied this system to human fetal lung-derived fibroblasts (TIG-1 cells) using six-well plates. Using MNPs, the transfected gene's expression level increased 2- to 4-fold under optimum conditions (Figure 4, unpublished data). Furthermore, to assess whether the multiple plasmids were expressed in a single cell, we attempt to induce the expression of three fluorescent proteins GFP, cyan fluorescent protein (CFP), and yellow fluorescent protein (YFP). Most cells expressed these three proteins (Figure 5, unpublished data) indicating that gene delivery using MNPs could introduce and allow expression of multiple genes in a single cell.

Figure 4. Optimum conditions for PEI max-MNPs magnetofection. To optimize conditions, we varied volume (**A**) and time on the magnetic plate (**B**). These results were evaluated by quantitative real-time RT-PCR. The relative expression level (*GFP/GAPDH*) in the human fetal lung-derived fibroblasts (TIG-1 cells) treated with PEI max alone (A), and in the absence of magnetic force (0 h) (B) was defined as 1. Optimal transfection conditions were established when TIG-1 cells were treated with 0.8 μg PEI max-MNPs and 2.0 μg pCAG-GFP for 8 h on the magnetic plate in either a six-well plate or a 35 mm dish. The asterisk (*) indicates a significant difference ($P < 0.05$).

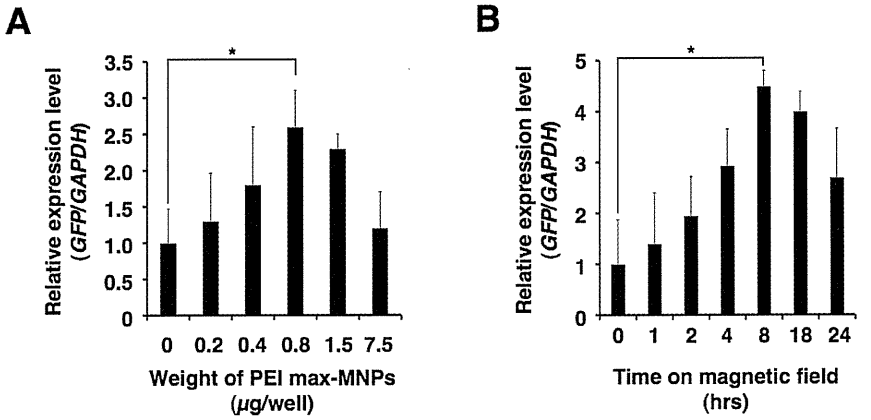

Table 3. Summary of magnetofection literature.

Author	Year	Vector	Magnetic Nanoparticles	Modifying Agent	Targeting Cell, or Tissue	TF Efficiency	Cell Viability (% of Control)	Reference
Kami D	2011	Plasmid	Iron oxide (γ-Fe_2O_3)	PEI max (MW: 25 k)	P19CL6	* 82%	100%	[107]
Pickard MR	2011	Plasmid	NeuroMag	-	Neural precursor cell	* 30%	70%	[39]
Hashimoto M	2011	Adenovirus, Biotin	SPION	PEI, Streptoavidin	HeLa	** 4-fold	-	[55]
		Adenovirus, Biotin	SPION	PEI, Streptoavidin	NIH3T3	** 10-fold	-	
		Adenovirus, Biotin	SPION	PEI, Streptoavidin	Mouse embryonic brain	-	-	
Biswas S	2011	Plasmid	Iron oxide (Fe_3O_4)	Aminooxy, Oxime ether	MCF-7	** 1425-fold	89%	[110]
B González	2011	Plasmid	SPION	Poly(propyleneimine) dendrimers	Saos-2 osteoblasts	* 12%	75%	[104]
Zhang H	2010	Plasmid	SPION	Branch PEI (MW: 25 k)	NIT3T3	* 64%	100%	[38]
		siRNA	SPION	Branch PEI (MW: 25 k)	NIT3T3	* 77%	100%	
Song HP	2010	Plasmid	PolyMag	Tat peptide	U251	* 60%	80%	[43]
		Plasmid	PolyMag	Tat peptide	Rat spinal cord	** 2-fold	-	
Arsianti M	2010	Plasmid	Iron oxide	Branch PEI (MW: 25 k)	BHK-21	-	60–90%	[51]
Shi Y	2010	Plasmid	Magnetite	Hyperbranch PEI (MW: 10 k)	COS-7	** 13-fold	-	[45]
Ang D	2010	Plasmid	Magnetite	Branch PEI (MW: 25 k)	COS-7	** 6-fold	70%	[46]
Tresilwised N	2010	Adenovirus	Iron oxide (Fe_2O_3, Fe_3O_4)	Branch PEI (MW: 25 k), Zonyl FSA fluorosurfactant	EPP85-181RDB	** 10-fold	-	[54]
Namgung R	2010	Plasmid	SPION	PEG, Branch PEI (MW: 25 k)	HUVEC	** 12-fold	80%	[48]
Yiu HH	2010	Plasmid	Iron oxide (Fe_3O_4)	PEI (MW: 25 k), MCM48 (Silica particle)	NCI-H292	** 4-fold	-	[49]
HC Wu	2010	Plasmid	Magnetite	Hydroxyapatite	Rat marrow stromal cells	* 60–70%	100%	[105]
Namiki Y	2009	Plasmid	Magnetite	Oleic acid, Phospholipid	HSC45	** 8-fold	-	[50]
		siRNA	Magnetite	Oleic acid, Phospholipid	Tissue sample from gastric cancer	-	-	
Kim TS	2009	Plasmid	PolyMag	-	Boar spermatozoa	-	-	[52]
Kievit FM	2009	Plasmid	SPION	PEI (MW: 25 k)	C6	* 90%	10%	[41]
		Plasmid	SPION	PEI (MW: 25 k), Chitosan	C6	* 45%	100%	
		Plasmid	PolyMag	-	C6	* 32%	66%	

Table 3. *Cont.*

Author	Year	Vector	Magnetic Nanoparticles	Modifying Agent	Targeting Cell, or Tissue	TF Efficiency	Cell Viability (% of Control)	Reference
Lee JH	2009	siRNA	MnMEIO	Serum albumin, PEG-RGD	MDA-MB-435-GFP	* 30%	-	[40]
Li Z	2009	Plasmid	Iron oxide	Poly-L-lysine	Lung tissue	*** 60%	-	[103]
Yang SY	2008	Plasmid	Iron oxide (Fe_3O_4)	Lipofectamine 2000	He99	-	-	[53]
		Plasmid	Iron oxide (Fe_3O_4)	DOTAP:DOPE	He99	-	-	
Pan X	2008	Plasmid	Magnetite	Oleic acid, Branch PEI (MW: 25 k), Transferrin	KB	** 300-fold	92%	[102]
Mykhaylyk O	2007	Plasmid	Iron oxide (Fe_2O_3, Fe_3O_4)	Branch PEI (MW: 25 k)	H441	* 49%	-	[42]
		Plasmid	Iron oxide (Fe_2O_3, Fe_3O_4)	Pluronic F-127	H441	* 37%	-	
		Plasmid	Iron oxide (Fe_2O_3, Fe_3O_4)	Lauroyl sarcosinate	H441	-	-	
		Plasmid	Iron oxide (Fe_2O_3, Fe_3O_4)	Branch PEI (MW: 25 k), Lauroyl sarcosinate	H441	-	-	
Morishita N	2005	Plasmid	Iron oxide (γFe_2O_3)	HVJ-E, protamine sulfate	BHK-21	** 4-fold	-	[47]
		Plasmid	Iron oxide (γ-Fe_2O_3)	HVJ-E, heparin sulfate	Liver, BALB/c mice (8 weeks age)	** 3-fold	-	
Scherer F	2002	Plasmid	SPION	PEI (MW: 800 k)	NIH3T3	** 5-fold	-	[44]
		Adenovirus	SPION	PEI (MW: 800 k)	K562	** 100-fold	-	
		Retrovirus	SPION	PEI (MW: 800 k)	NIH3T3	* 20%	-	
Mah C	2002	Adenovirus	Avidinylated magnetite	Biotunylated heparan sulfate	C12S	* 75%	-	[56]
		Adenovirus	Avidinylated magnetite	Biotunylated heparan sulfate	Adult 129/SvJ mice	-	-	

* indicates % of fluorescent positive cells analyzed by flow cytometric analysis.

** indicates analysis by luciferase activity assay compared with control. Transfection efficiency was indicated optimal transfection condition.

*** indicates transfection without magnetic force.

PEI: Polyethylenimine; PEI max: Deacaylated PEI; MNP: Magnetic nanoparticle; SPION: Superparamagnetic iron oxide nanoparticle; MW: Molecular weight; TF: transfection; PolyMag: Commercial Magnetofection reagent), NeuroMag (Commercial Magnetofection reagent); HVJ-E: hemagglutinating virus of Japan-envelope; DOTAP: 1,2-dioleoyl- 3-trimethylammonium-propane; DOPE: 1,2-dioleoyl-3-sn- phosphatidyl-ethanolamine; Tat peptide: cationic cell penetrating peptide; MeMEIO: Manganese-doped magnetism-engineered iron oxide; PEG: polyethylene glycol, Zonyl FSA fluorosurfactant: Lithium 3-[2-(perfluoroalkyl)ethylthio]propionate).

Figure 5. Transfection of TIG-1 cells with multiple genes using PEI max-MNPs. TIG-1 cells were simultaneously transfected with GFP, CFP, and YFP expression vector plasmids. TIG-1 cells were treated with 0.8 μg of PEI max-MNPs and 0.7 μg each of pCAG-GFP (GFP, provided by Dr. Nishino), pPhi-Yellow-N (YFP, Evrogen), and pAmCyan1-C1 (CFP, Clonetech) for 8 h on the magnetic plate in a six-well plate or a 35 mm dish. White bar indicates 200 μm.

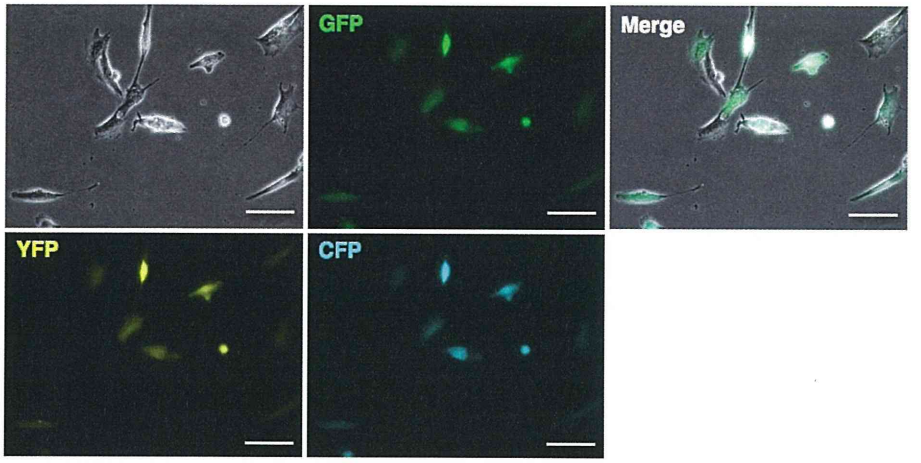

5. Conclusions

The great promise of gene therapy for treating devastating, incurable diseases has yet to be realized. Less toxic and more efficient systems will be required, and robust research efforts in this regard are currently underway. Rapid advances have been made in adapting nanoparticle technology for basic biomedical and clinical research. Nanoparticles are already being used clinically to enhance MRI imaging, and drug delivery for cancer patients. Our own research has focused on gene delivery systems for autologous cell transplantation therapy, in which the patient's own cells are transfected with the gene required to correct their condition. In particular, our laboratory and those of others have aimed to optimize magnetofection by developing better nanoparticle coating agents [38,40–51,53–55]. Nanoparticle size is another important parameter but there were few reports addressing this subject [111]. Since cells endocytose MNPs [51,100,101], MNP size has significant implications for transfection efficiency. PEI-MNPs forms magnetoplex, which increased its influence on the magnetic force. Furthermore, MNP size influences cytotoxicity [112], and more studies on this aspect of MNP technology will be crucial for enhancing transfection efficiencies.

The two research groups reported the important developments in the field of magnetofection. The first is the influence of the oscillating magnetic force on transfection [113,114]. The second is the use of MNP-heating, and -transfection [15,16]. The purpose of these studies have increased the efficiency of transfection, and/or induced a fever by oscillating MNPs for hyperthermia. The latter, a combination of MNP-heating and -transfection, was expected to research the efficacy of both hyperthermia and gene delivery. In the future, the studies of magnetofection using the oscillating MNPs could be developed as a novel methodology.

We found that PEI is an excellent cationic polymer for dispersing MNPs and that its water solubility, stability, and low toxicity contribute to enhancing transfection efficiency [95,115–119].